MECHANICAL

TECHNOLOGY

INCORPORATED

Mechanical Technology Incorporated
968 Albany Shaker Road
Latham, New York 12110

MTI-69TR16

ON THE START-UP PROCESS IN A GASEOUS SQUEEZE-FILM THRUST CIRCULAR DISK

by

T. Chiang
C.H.T. Pan
V. Castelli

Mechanical Technology Incorporated
968 Albany Shaker Road
Latham, New York 12110

MTI-69TR16

ON THE START-UP PROCESS IN A GASEOUS SQUEEZE-FILM THRUST CIRCULAR DISK

by

T. Chiang
C.H.T. Pan
V. Castelli

NO. MTI-69TR16

DATE: April, 1969

TECHNICAL REPORT

ON THE START-UP PROCESS IN A GASEOUS SQUEEZE-FILM THRUST CIRCULAR DISK

by
T. Chiang
C.H.T. Pan
V. Castelli

T. Chiang C.H.T. Pan Vittorio Castelli

Author (s)

Walter A. Shaw

Approved

Approved

Prepared for

National Aeronautics and Space Administration
George C. Marshall Space Flight Center
Huntsville, Alabama

Prepared under

Contract: NAS 8-11678

MECHANICAL TECHNOLOGY INCORPORATED

968 ALBANY - SHAKER ROAD — LATHAM, NEW YORK — PHONE 785-0922

TABLE OF CONTENTS

INTRODUCTION

In a gaseous squeeze-film bearing, one of the bearing surfaces driven by a transducer, oscillates at a high frequency and an amplitude not small compared to the mean film thickness. This generates load supporting capabilities. In the literature, most of the analytical and experimental works concentrated on the load capacity and stiffness of squeeze-film bearings after a steady-state oscillation has been reached [Ref. 1 to 4].

In most circumstances a squeeze-film thrust bearing is started by first having the supported mass (the float) resting on the lower bearing surface. One then turns on the transducer which drives the lower squeeze surface. At first, there is a high pitch noise in addition to the noise generated by the transducer structure if the squeeze frequency is in the audible range. The high-pitch noise caused by solid contact between bearing surfaces during the initial stage of the starting process, will suddenly disappear, indicating that a film has been maintained. The physical starting process as described above, is therefore, very complicated. A simplified model will be considered in the analysis.

ANALYSIS

Consider a squeeze-film thrust plate shown in Fig. 1. The lower plate, driven by a transducer, is squeezing at an amplitude e which could be a function of time because it takes a certain amount of time for the transducer to build up and reach a steady-state amplitude. If we start the bearing with the float resting on the lower squeeze surface, the excursion amplitude takes even longer to build up because of the interfacial damping. For a given squeeze frequency Ω and as the excursion amplitude e increases, it will reach a point that $e\Omega^2$ is equal to the gravitational acceleration (or that due to preloading if the float is preloaded). From that point on, the supported mass will not be able to follow the lower squeeze surface during a downward motion; the squeeze surfaces will momentarily seperate. Several possible things or their combination may occur at this stage of the starting process; they are enumerated as follows:

1) If the time interval of seperation is very short, the squeeze-film pressure has no time to build up. Therefore, the lower squeeze surface will "hit" the float at an impact velocity depending on the particular dynamic condition.

2) After impact, they may stick together until they seperate again by the aforementioned mechanism, or the float may be bounced off by the laws of dynamics. Because the impact causes some internal losses, the excursion amplitude decreases somewhat, and then increases again afterward.

3) The above process will repeat until the float is either throsn up or bounced up to a height of, say, 5 times the equilibrium film thickness. It is from this point that we shall start the analysis of the start-up process of a squeeze-film thrust bearing.

The film thickness can be considered to consist of the following,

$$h(t) = e(t) \cos \Omega t + h_\infty(t) \qquad (1)$$

The first term on the right hand side of (1) is obviously the squeeze motion, whereas the second term $h_\infty(t)$ is the transient film thickness. Obviously, $h_\infty(t)$ indicates the location of the supported mass; as $t \to \infty$, $h_\infty(t) \to C$ which is the equilibrium film thickness.

The isothermal Reynolds' equation of a squeeze-film thrust circular disk can be written as

$$\frac{1}{R}\frac{\partial}{\partial R}\left(PH^3 R \frac{\partial P}{\partial R}\right) = \frac{12\mu}{p_a}\left(\frac{r_o}{C}\right)^2 \frac{\partial \psi}{\partial t} \tag{2}$$

where

$$\left.\begin{aligned} P &= p/p_a \\ H &= h/C \\ \psi &= PH \\ R &= r/r_o \\ C &= \text{steady-state equilibrium film thickness} \end{aligned}\right] \tag{3}$$

Note that in Eq. (2) the only two dimensional quantities are t and $12\mu/p_a\,(r_o/C)^2$, the latter has the physical significance of a transient time. For convenience, we define a characteristic frequency ω,

$$\omega \equiv \left[\frac{12\mu}{p_a}\left(\frac{r_o}{C}\right)^2\right]^{-1} \tag{4}$$

The initial and boundary conditions for Eq. (2) are

$$\left.\begin{aligned} P &= 1 \quad \text{at} \quad R = 1 \\ \frac{\partial P}{\partial R} &= 0 \quad \text{at} \quad R = 0 \\ P &= 1 \quad \text{at} \quad t = 0 \end{aligned}\right] \tag{5}$$

The variation of e with t is dependent on the characteristics of the driving transducer. A typical plot of e versus t is shown in Fig. 2. In most circumstances it can best be represented by

$$\frac{e}{e_a} = 1 - \exp(-t/t_1) \tag{6}$$

where e_a is the asymptotic value of e and t_1 is a relaxation time.

Since both the squeeze action and transient nature of the problem contribute to the time dependence, we can write formally

$$\psi(r,t) = \psi(R,T,\tau) \tag{7}$$

where

$$\left.\begin{aligned} T &= \omega t \\ \tau &= \Omega t \end{aligned}\right] \tag{8}$$

Thus,

$$\frac{\partial \psi}{\partial t} = \frac{\partial \psi}{\partial \tau}\frac{d\tau}{dt} + \frac{\partial \psi}{\partial T}\frac{dT}{dt} \tag{9}$$

Substitute into Eq. (2),

$$\frac{H}{2}\frac{1}{R}\frac{\partial}{\partial R}\left(R\frac{\partial \psi}{\partial R}^2\right) = \sigma\frac{\partial \psi}{\partial \tau} + \frac{\partial \psi}{\partial T} \tag{10}$$

where σ = squeeze number

$$= \frac{12\mu\Omega}{p_a}\left(\frac{r_o}{C}\right)^2 = \frac{\Omega}{\omega} \tag{11}$$

It is seen from Eq. (8) that there are two time scales for this problem, one is associated with the squeezing and the other is associated with the transient behavior. Typically, Ω is much greater than ω. Thus,

$$\frac{T}{\tau} = \frac{\omega}{\Omega} \ll 1 \tag{12}$$

Now, it is quite obvious that when the squeeze motion completes one cycle (τ changes from τ_o to $\tau_o + 2\pi$), the transient time changes only by an amount equal to $2\pi\ \omega/\Omega$ which approaches zero as $\Omega \to \infty$. Therefore, the transient motion is quasi-stationary with respect to the high frequency squeeze motion. A general asymptotic analysis for large σ (or Ω) was given in [ ] and [ ]. The results will be applied to the present problem and summarized as follows.

$$\text{As } \sigma \to \infty,\ \psi(R,T,\tau) \to \psi_\infty(R,T) \tag{13}$$

where ψ_∞ is the asymptotic approximation of ψ for large σ in the interior of the bearing film, i.e. The whole film excluding the narrow region near the edge (R=1). This narrow region is the boundary layer of the squeeze film and is of the order of $1/\sqrt{\sigma}$.

Using the results of [ ] and [ ], the governing equation of ψ_∞ can be shown to be

$$\frac{1}{2R}\ \frac{\partial}{\partial R}\left[R\ \frac{\partial(H_\infty \psi_\infty^{\,2})}{\partial R}\right] = \frac{\partial \psi_\infty}{\partial T} \tag{14}$$

with boundary conditions

$$\psi_\infty^{\,2}\Big|_{R=1} = H_\infty^{\,2}(T) + \frac{3}{2}\ \epsilon^2(T) \tag{15}$$

$$\frac{\partial}{\partial R}(\psi_\infty^{\,2})\Big|_{R=0} = 0 \tag{16}$$

and initial condition

$$\psi_\infty\Big|_{T=0} = H_\infty\Big|_{T=0} \tag{17}$$

where

$$\epsilon(T) = \frac{e(T)}{C} \tag{18}$$

Eq. (1) has been non-dimensionalized to

$$H(T,\tau) = H_\infty(T) + \epsilon(T)\cos\tau \tag{19}$$

Note that

$$\int_0^{2\pi} H(T,\tau)d\tau = H_\infty(T) \tag{20}$$

In Eq. (14) there are two unknowns, H_∞ and ψ_∞. We can write an additional equation which is the equation of motion of the supported mass.

$$M\frac{d^2h_\infty}{dt^2} = -Mg + \int_0^{r_o}(p - p_a)\,2\pi r dr$$

or

$$\frac{MC\omega^2}{p_aA}\frac{d^2H_\infty}{dT^2} = -\frac{Mg}{p_aA} + 2\int_0^1 \left(\frac{\psi_\infty}{H} - 1\right) RdR \tag{21}$$

Integrate Eq. (21) over one squeeze cycle,

$$B\frac{d^2H_\infty}{dT^2} = -\frac{Mg}{p_aA} - 1 + 2\int_0^{2\pi}\frac{d\tau}{2\pi}\int_0^1 \frac{\psi_\infty}{H}\,RdR \tag{22}$$

where

$$B = \frac{MC\omega^2}{p_aA}$$

We have used the condition that H_∞ and hence d^2H_∞/dT^2 are independent of τ.

Now, if we let

$$G(R,T) = \psi_\infty^2(R,T) \tag{23}$$

then, Eq. (14) is reduced to

$$\frac{\partial^2 G}{\partial R^2} + \frac{1}{R}\frac{\partial G}{\partial R} = \frac{1}{H_\infty \sqrt{G}}\frac{\partial G}{\partial T} \tag{24}$$

The boundary and initial conditions are, from Eqs. (15) to (17),

$$G(R=1,\ T) = H_\infty^2(T) + \frac{3}{2}e^2(T) \tag{25}$$

$$\left.\frac{\partial G}{\partial R}\right|_{R=0} = 0 \tag{26}$$

$$G(R,T=0) = H_\infty^2(T=0) \tag{27}$$

Carry out the τ integration and replace ψ_∞ by G,

$$B\frac{d^2 H_\infty}{dT^2} = -\frac{Mg}{p_a A} - 1 + \frac{2}{\sqrt{H_\infty^2(T) - e^2(T)}}\int_0^1 \sqrt{G}\ RdR \tag{28}$$

One can easily prescribe two initial conditions $H_\infty(T=0)$ and $\dot{H}_\infty(T=0)$ corresponding to the initial displacement and velocity respectively.

Equations (24) and (28) are to be solved for H_∞ and G by numerical methods in the next section. It is interesting to note here that when steady state is reached, both H_∞ and G will be independent of T; in fact, H_∞ should be unity by definition. Let subscript "ss" indicate steady state solutions. Then, we have

$$\frac{d^2G_{ss}}{dR^2} + \frac{1}{R}\frac{dG_{ss}}{dR} = 0 \tag{29}$$

and

$$Q_{ss} - \frac{Mg}{p_a A} - 1 = 0 \tag{30}$$

where

$$\left.\begin{aligned} Q &\equiv \sqrt{\frac{2}{H_\infty^{\dagger}(T) - \epsilon^2(T)}} \int_0^1 \sqrt{G}\, RdR \\ &= \text{normalized squeeze-film force} \\ Q_{ss} &= \sqrt{\frac{2}{1-\epsilon^2}} \int_0^1 \sqrt{G_{ss}}\, RdR \end{aligned}\right\} \tag{31}$$

The solution of (29) satisfying (25) and (26) can be shown to be

$$G_{ss} = 1 + \frac{3}{2}\epsilon^2 \tag{32}$$

Note that G_{ss} is independent of R. From Eq. (31) we can easily obtain the steady-state normalized squeeze-film force,

$$Q_{ss} = \sqrt{\frac{1 + \frac{3}{2}\epsilon^2}{1 - \epsilon^2}} \tag{33}$$

which is a well known result.

During the transient period, G and H_∞ have to be solved from Eq. (24) and (28), from which the instantaneous squeeze-film force Q can be calculated.

RESULTS AND DISCUSSIONS

A numerical analysis for solving Eqs. (24) and (28) subject to boundary and initial conditions (25), (26) and (27) and initial H_∞ and $\dot{H}_\infty$, is shown in Appendix I. The numerical computation has been programmed on a computer. We shall illustrate the results by the following example.

Given:

$r_o = 1$ in.

$M = 0.5$ lb.

$t_1 = 0$

$e = e_a = 0.0005$ in.

$\mu = 2.7 \times 10^{-9}$ lb.sec/in^2

$p_a = 14.7$ psi.

The equilibrium film thickness can be readily calculated from (30)and (33).

$C = 0.00538$ in.

The characteristic frequency ω defined in (4) is calculated to be $\omega = 13100$ rad/sec. This value of ω is obviously on its high side because C is normally designed at 1 mil (e can be reduced accordingly). With C = 0.001 in, $\omega = 452$ rad/sec. which is much lower than the previous value.

If we set $H_\infty(T=0) = 10$, $\dot{H}_\infty(T=0) = 0$, the variations of G at R = 0 and R = 1, against T, are shown in Fig. 3. Recall that $G = \psi_\infty^2 = P^2 H_\infty^2$. When H_∞ is large (say 5), $P \approx 1$; hence $G \approx H_\infty^2$. Furthermore, this indicates that when H_∞ is large G does not vary appreciably along the film. When H_∞ is small (less than 1), the spatial distribution of G is shown in Fig. 4. The G curves for various T in Fig. 4 give an

indication of the distribution of P^2 at different time, noting that $P^2 = G/H_\infty^2$. The dimensionless squeeze-film force Q can now be obtained from G by quadrature. In Fig. 5 H_∞ and Q are plotted T. It is seen that the supported mass starts with a zero velocity and an elevation of ten C. Since the pressure inside the film is essentially ambient, the mass falls down freely until $H_\infty \approx 1$ ($T \approx 200$). There the pressure starts to build up as indicated by increasing Q in Fig. 5. Consequently, the mass slows down to a zero velocity at T = 216 and $H_\infty = 0.21$. The value of Q is 1.45 at $H_\infty = 0.21$, which is much higher than the steady-state force required to maintain equilibrium (which is 1.01). Therefore, the mass will be pushed upward and come down again. The process will repeat itself with decreasing amplitude, until finally it will reach a steady-state situation. The solution has been carried to T = 1000. With ω = 13,100 rad/sec, this corresponds to a real time of t = 0.076 sec. only; it is already clear that the mass is approaching to the equilibrium position. If the same mass is displaced to $H_\infty(T=0) = 5$ and $\dot{H}_\infty(T=0) = 0$, the solution H_∞ is plotted against T in Fig. 6. The two H_∞ curves in Fig. 6 show similar characteristics.

Let the point A in Fig. 5 be at T = 205, $H_\infty = 1.0$ and $\dot{H}_\infty = -0.0803$. It is interesting to note that if we prescribe the initial conditions of $H_\infty = 1.0$ and $\dot{H}_\infty = -0.0803$, and run the computer program, the solution would follow precisely the same path from point "A" on, as can be anticipated. The above situation can be interpreted as exerting an impulsive force on a mass supported by a squeeze-film bearing. Suppose that the impulsive force yields a velocity of $\dot{H}_\infty = -0.0803$ (or 5.6 in/sec.) at $H_\infty = 1$. Then the solution obviously indicates that the squeeze-film bearing would survive the shock and eventually restore to its steady operation.

It is also interesting to observe that the fundamental of the oscillations of H_∞ displayed in Figures 5 and 6, has a period of approximately 210 (or t = 0.016 sec.). In other words, there is a fundamental frequency of 62 cps. This is obviously the $\sqrt{k/m}$ type oscillation. The dependence of the squeeze-film stiffness k on H_∞ is schematically shown in the following sketch. Although k is not a constant, for the purpose of calculating the natural frequency we take the value of k at $H_\infty = 1$ in as much as the oscillations are more or less centered

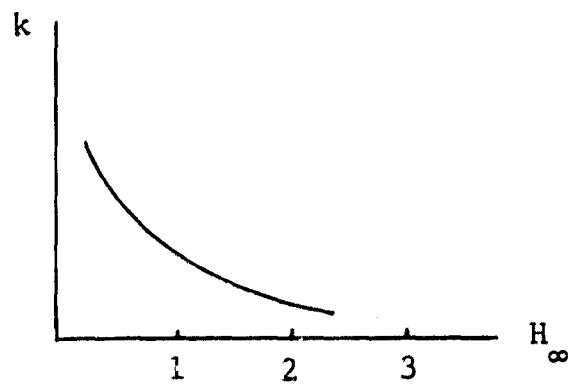

at $H_\infty = 1$. Thus, $\sqrt{\frac{k}{m}} = \sqrt{\frac{214}{0.5/386}} = 406$ rad/sec. = 65 cps. which agrees quite well with the fundamental frequency displayed in Fig. 5. Note that we have used the value of the static stiffness for k instead of the dynamic stiffness. Since the frequency of oscillation is low (65 cps), the quasi-static value of the stiffness should be a good approximation (See Ref. 7).

SUMMARY

The start-up process of a squeeze-film thrust bearing was analyzed with the simplification that the float starts off with a given velocity and a given elevation different from the equilibrium film thickness.

Since the time scale involved in the transient process is much longer than the squeeze period, one can apply a generalized asymptotic analysis for large σ. The results show that when the gap is greater than the equilibrium film thickness C, the squeeze-film force is not large enough to support the float; consequently, the gap would decrease. When the gap decreases to a value equal to C, it will continue to decrease because of the inertia of the float. But now the squeeze-film force is building up until it reaches a value that will compensate the float inertia; at that point, the gap ceases to decrease. The squeeze-film force is now too large and the float starts to move up. It will over-shoot the equilibrium position and the process will repeat itself in a convergent manner. Eventually, the float would settle down at the equilibrium position.

APPENDIX I
NUMERICAL ANALYSIS

The numerical solution of Eqs. (24) and (28) subject to boundary and initial conditions (25), (26) and (27) and initial H_∞ and $\dot{H}_\infty$, will be obtained in this section. First, let us rewrite Eq. (28) in the following form.

$$\ddot{H}_\infty(T) = \frac{-\frac{Mg}{p_a A} - 1 + 2\left[H_\infty^2(T) - \varepsilon^2(T)\right]^{-1/2} \int_0^1 \sqrt{G(R,T)}\, R\,dR}{B} \qquad (I.1)$$

Let ΔT be the time step. We can integrate (I.1) to obtain $\dot{H}_\infty$ and H_∞ at $T + \Delta T$.

$$\dot{H}_\infty(T + \Delta T) = \dot{H}_\infty(T) + \ddot{H}_\infty(T)\,\Delta T \qquad (I.2)$$

$$H_\infty(T + \Delta T) = H_\infty(T) + \dot{H}_\infty(T + \Delta T)\,\Delta T \qquad (I.3)$$

In order to achieve numerical stability, implicit method will be used in solving Eq. (24) which can be written as

$$\frac{G_i(T + \Delta T) - G_i(T)}{\Delta T} = \left[\frac{\partial^2 G_i}{\partial R^2} + \frac{1}{R_i}\frac{\partial G_i}{\partial R}\right]_{T + \Delta T} H_\infty(T)\sqrt{G_i(T)} \qquad (I.4)$$

Note that the space derivatives of G are evaluated at $T + \Delta T$, whereas the explicit method evaluates the space derivatives at T. The subscript "i" indicates stations. Let there be N divisions between R = 0 and 1, so that

$$\Delta R = \frac{1}{N} \qquad (I.5)$$

Using central difference formula we have

$$\frac{\partial G_i}{\partial R} = \frac{G_{i+1} - G_{i-1}}{2\Delta R} \qquad (I.6)$$

$$\frac{\partial^2 G_i}{\partial R^2} = \frac{G_{i+1} - 2G_i + G_{i-1}}{(\Delta R)^2} \qquad (I.7)$$

Substitute into (I.4),

$$\frac{G_i(T + \Delta T)}{\Delta T} - \left[\frac{G_{i+1}(T + \Delta T) - 2G_i(T + \Delta T) + G_{i-1}(T + \Delta T)}{(\Delta R)^2} + \frac{G_{i+1}(T + \Delta T) - G_{i-1}(T + \Delta T)}{2R_i \Delta R} \right] H_\infty(T) \sqrt{G_i(T)}$$

$$= \frac{G_i(T)}{\Delta T} \qquad (i = 1, 2, \ldots N - 1) \qquad (I.8)$$

The boundary condition (25) can be written as

$$G_N(T) = H_\infty^2(T) + \frac{3}{2} \epsilon^2(T) \qquad (I.9)$$

The qero-slope condition (26) at R = 0 can be rearranged so that we can use it more effectively than writing $G_0(T) = G_1(T)$. We first note that near R = 0 we can approximate G by a parabola.

$$G = aR^2 + b \qquad \text{(for small R)}$$

Then it is clear that

$$\frac{1}{R}\left.\frac{\partial G}{\partial R}\right|_{R=0} = \left.\frac{\partial^2 G}{\partial R^2}\right|_{R=0} = 2a$$

and

$$\left.\frac{\partial^2 G}{\partial R^2}\right|_{R=0} = \frac{G_1 - 2G_0 + G_{-1}}{(\Delta R)^2} = 2\,\frac{G_1 - G_0}{(\Delta R)^2}$$

Utilizing (24), we can replace the qero-slope condition by

$$\frac{G_0(T+\Delta T)}{\Delta T} - \frac{4}{(\Delta R)^2}\,H_\infty(T)\,\sqrt{G_0(T)}\,\left[G_1(T+\Delta T) - G_0(T+\Delta T)\right] = \frac{G_0(T)}{\Delta T} \qquad \text{(I.10)}$$

The initial conditions for the system are

$$G(R,T=0) = H_\infty^{\,2}(T=0) \qquad \text{(I.11)}$$

$$\left.\begin{aligned} H_\infty(T=0) &= \text{given} \\ &\cdot \\ H_\infty(T=0) &= \text{given} \end{aligned}\right] \qquad \text{(I.12)}$$

Knowing the initial values of G's and H_∞, we can start the process by marching one time step ΔT from T=0, and calculating $H_\infty(\Delta T)$ from (I.1), (I.2) and (I.3). There are "N+1" unknown G's at ΔT, i.e., G_0, G_1, . . . G_N. Equation (I.8) provides "N-1" equations. Equations (I.9) and (I.10) give two additional equations. Thus, the "N+1" equations can be solved simultaneously for G_0, G_1, . . . G_N at ΔT. We can repeat the process at each time step progressively until a prescribed time has been reached.

REFERENCES

1. Pan, C.H.T., "On Asymptotic Analysis of Gaseous Squeeze-Film Bearings", Journal of Lubrication Technology, Trans. of ASME, Vol. 89, Series F, No. 3, July 1967, p. 245.

2. Pan, C.H.T., Malanoski, S.B., Broussard, Jr., P.H and Burch, J.L., "Theory and Experiments of Squeeze-Film Gas Bearings - Part 1 Cylindrical Journal Bearing," Journal Basic Eng., Trans. ASME, Vol. 88, Series D, No. 1, March 1966, p. 191.

3. Chiang, T., Malanoski, S.B. and Pan, C.H.T., "Spherical Squeeze-Film Hybrid Bearing with Small Steady-State Radial Displacement," Journal of Lubrication Technology, Trans. of ASME, Vol. 89, Series F, No. 3, July 1967, p. 254.

4. Beck, J.V. and Strodtman, C.L., "Load Support of the Squeeze-Film Journal Bearing of Finite Length," Journal of Lubrication Technology, Trans. ASME, Vol. 90, Series F, No. 1, January 1968, p. 157.

5. Elrod, H.G., "A Differential Equation for Dynamic Operation of Squeeze-Film Bearings", presented at the Third Bi-annual Gas Bearing Symposium, University of Southampton, 1967.

6. Chiang, T., Pan, C.H.T., and Elrod, H.G., "Dynamic Response of a Double Squeeze-Film Thrust Plate," MTI Report 68TR56.

7. Pan, C.H.T. and Chiang, T., "Dynamic Behavior of the Spherical Squeeze-Film Hybrid Bearing", Journal of Lubrication Technology, Trans. of ASME, Vol. 91, Series F, No. 1, January 1969, p. 149.

NOMENCLATURE

A	area of squeeze-film
B	mass parameter
C	equilibrium film thickness
e	squeeze amplitude
e_a	asymptotic value of e
G	ψ_∞^2
h	instantaneous film thickness
h_∞	time-average of h over one squeeze cycle, h_∞ also indicates the location of the supported mass
H	h/C
H_∞	h_∞/C
M	mass supported by squeeze-film
p	pressure
p_a	ambient pressure
P	p/p_a
Q	normalized squeeze-film force, Eq. (31)
Q_{ss}	steady-state Q
r	radial coordinate
r_o	outer radius of circular plate
R	r/r_o
t	time
t_1	relaxation time defined in Eq. (6)
T	dimensionless time, ωt

NOMENCLATURE (Continued)

ε	e/C
μ	viscosity
σ	squeeze number
τ	Ωt
ψ	PH
ϖ	typical frequency defined in Eq. (4)
Ω	squeeze frequency

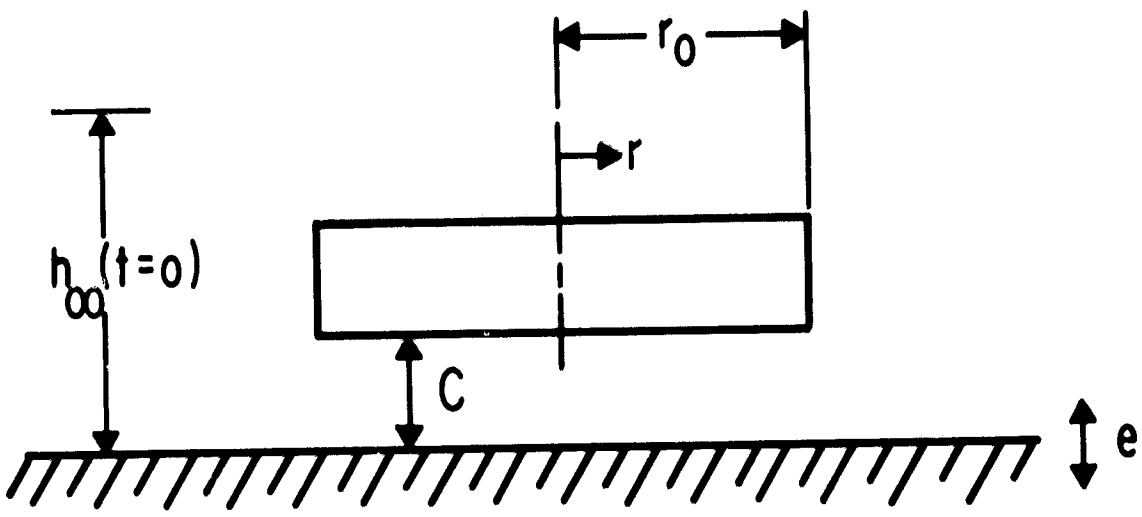

Fig. 1 Geometry of a Squeeze-Film Thrust Plate

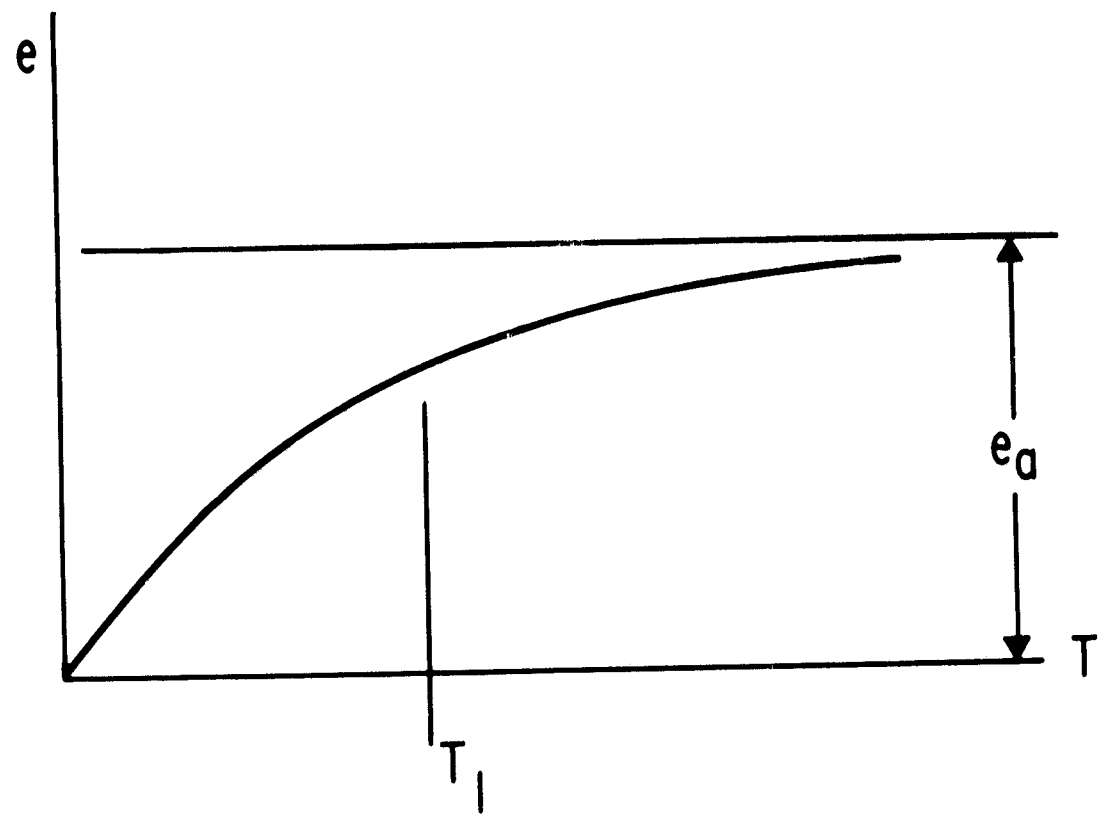

Fig. 2 Squeeze Amplitude Versus Time

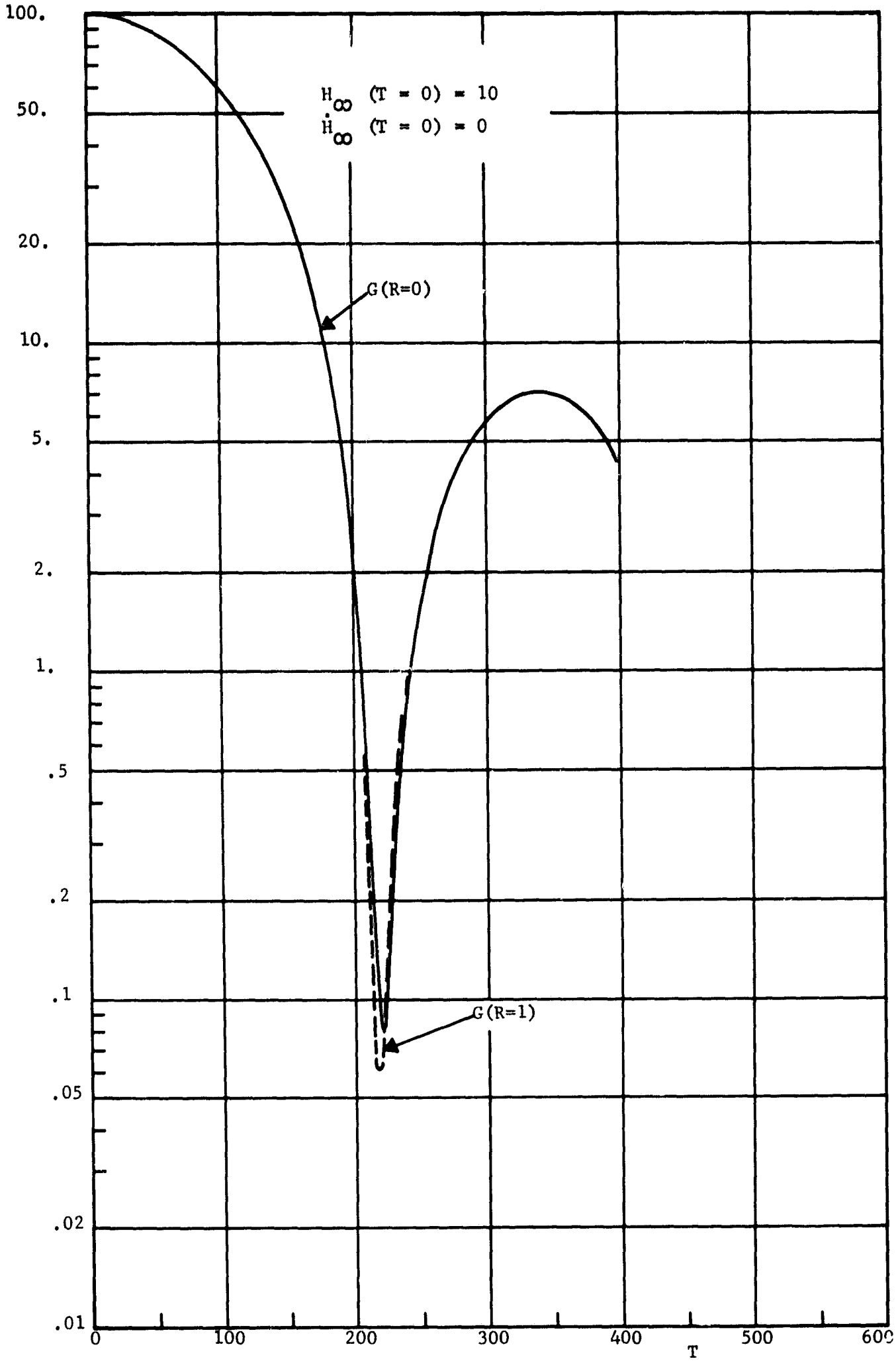

Fig. 3 G-Function Versus Dimensionless Time

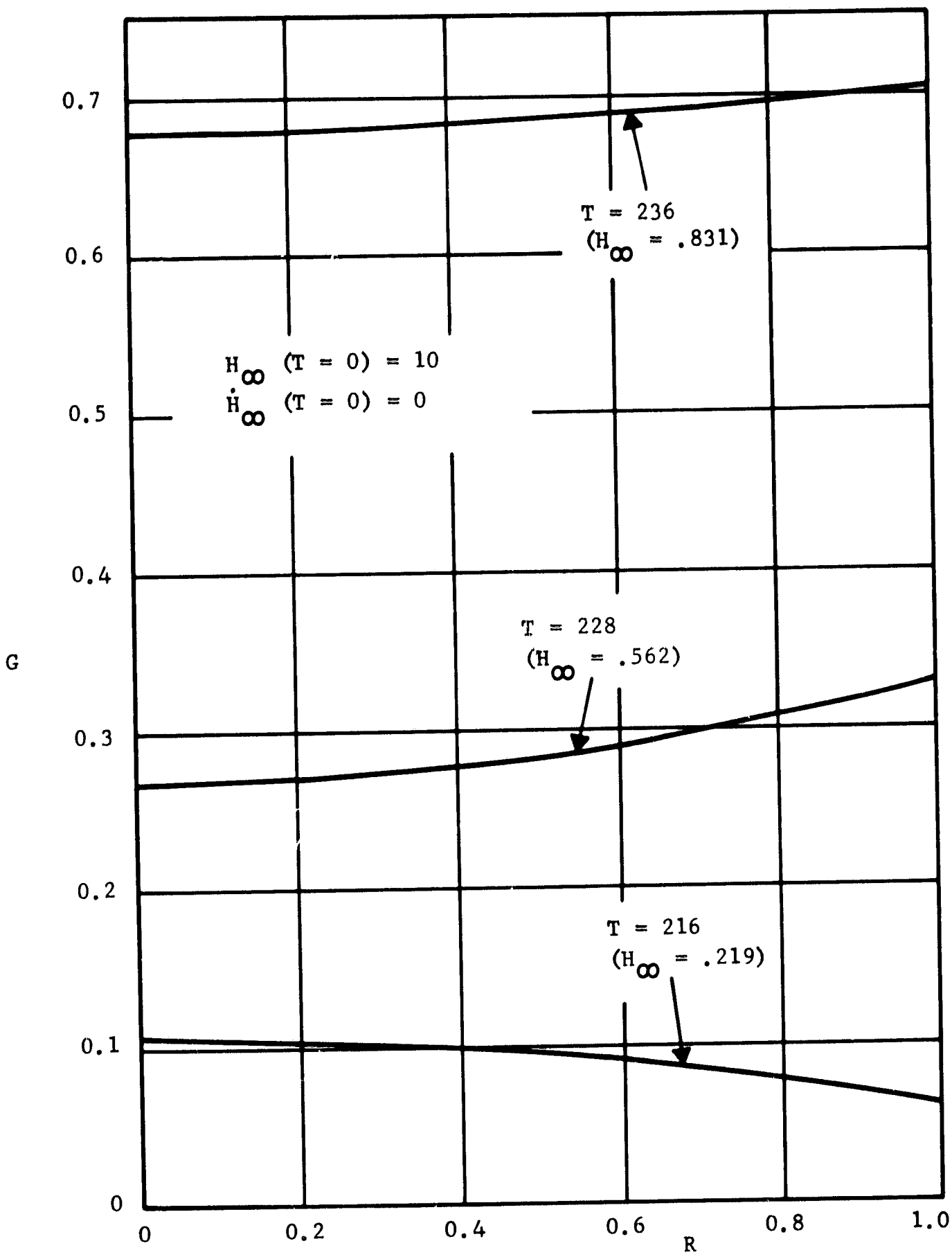

Fig. 4 Distributions of G at Various T

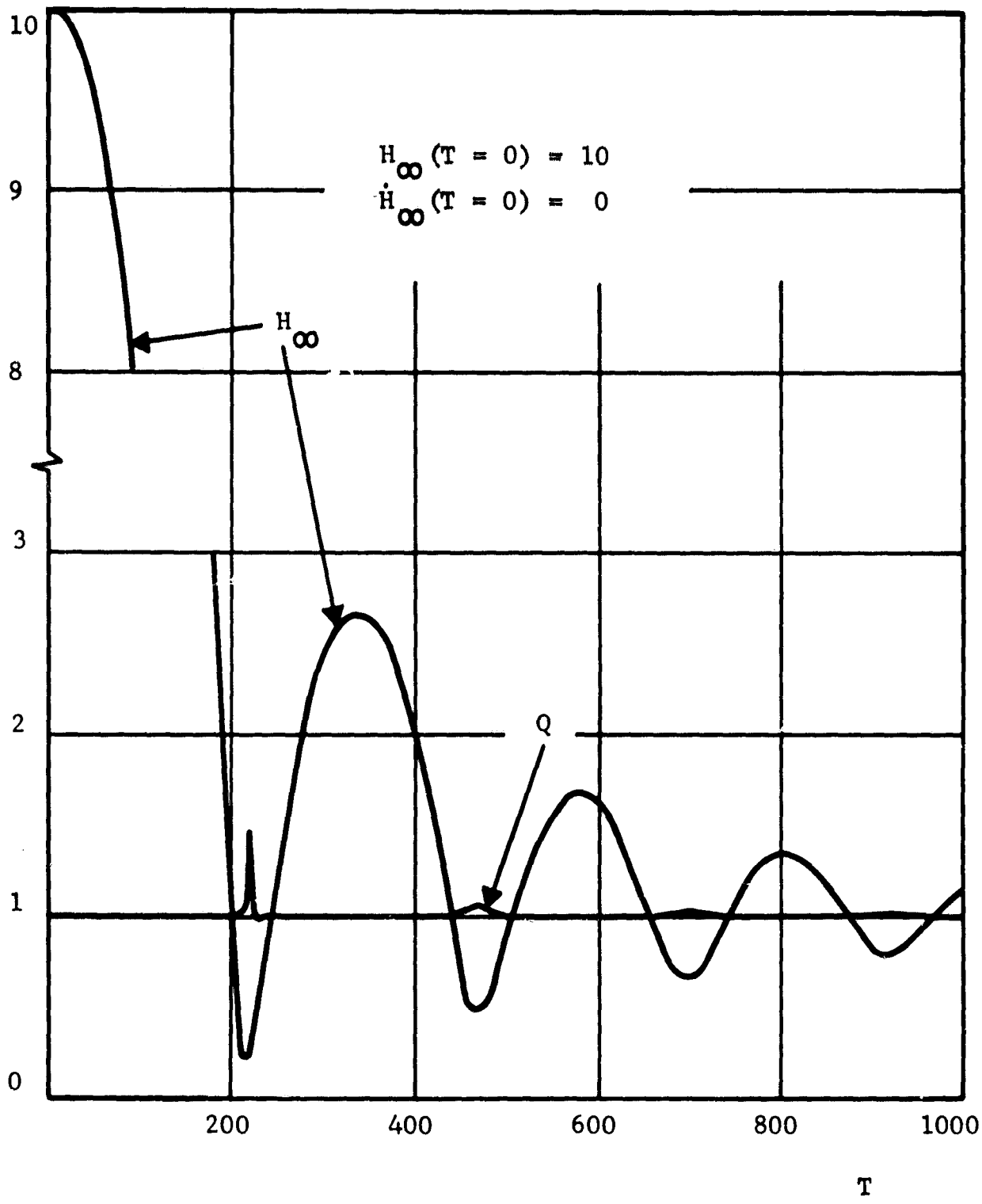

Fig. 5 Dimensionless Film Thickness and Squeeze-Film Force Versus T

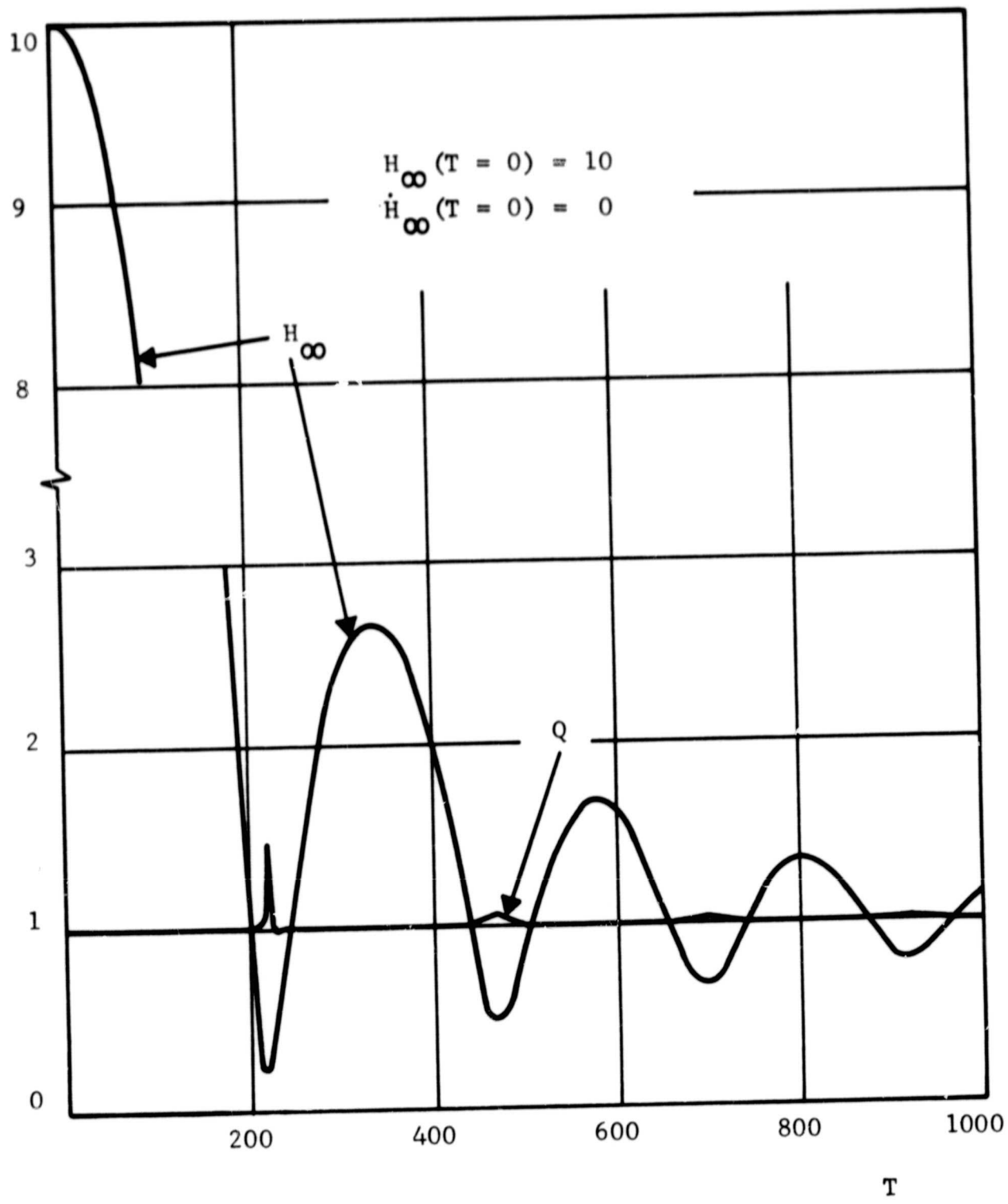

Fig. 5 Dimensionless Film Thickness and Squeeze-Film Force Versus T

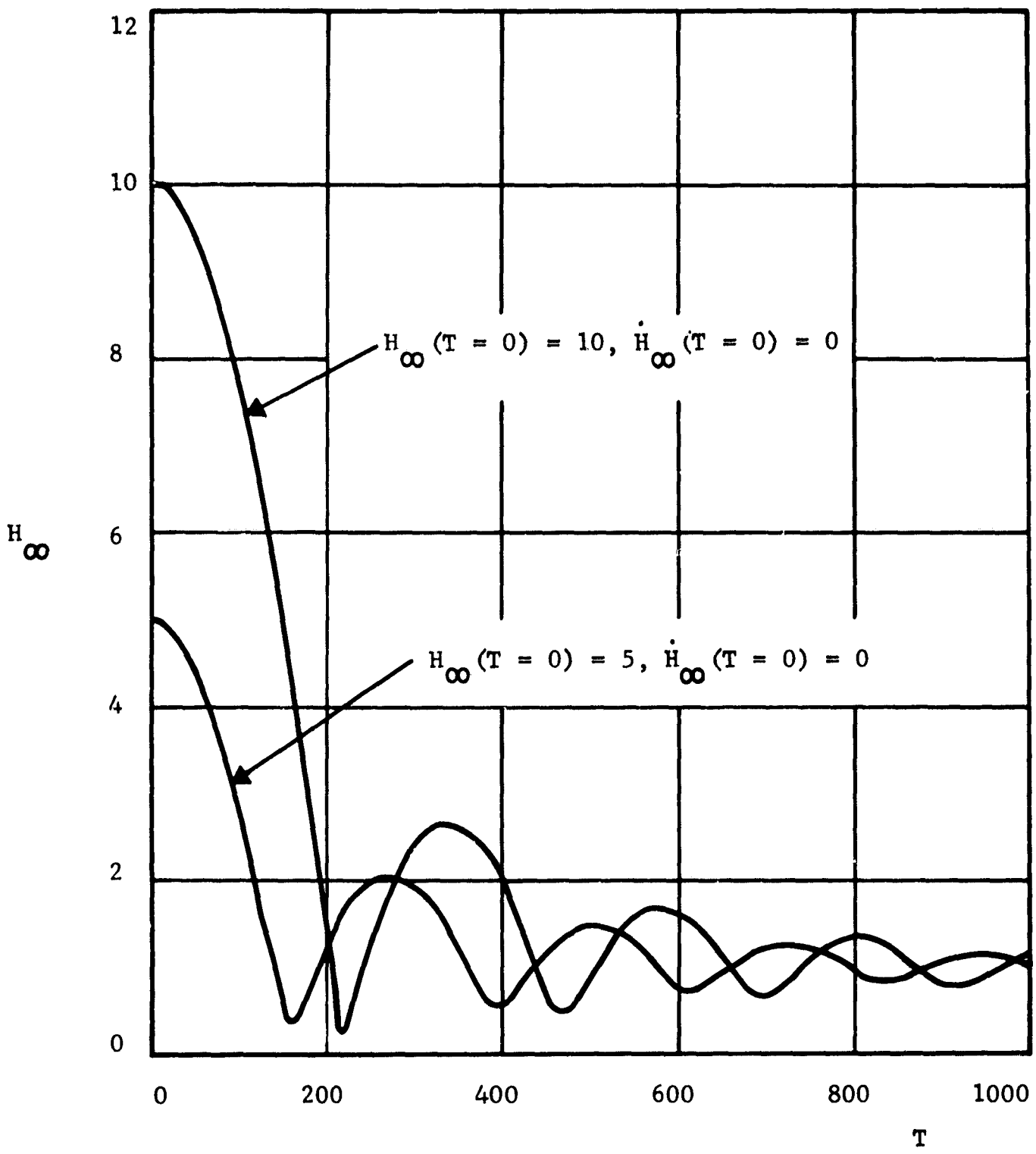

Fig. 6 Dimensionless Film Thicknesses Versus T